Published in final edited form as:
Int J Dev Biol. 2014 ; 58(5): 325–333. doi:10.1387/ijdb.130327cm.

α integrin cytoplasmic tails have tissue-specific roles during *C. elegans* development

CHRISTOPHER M. MEIGHAN[1,*] and **JEAN E. SCHWARZBAUER**[2]

[1]Department of Molecular Biology and Chemistry, Christopher Newport University, Newport News, VA, USA

[2]Department of Molecular Biology, Princeton University, Princeton, NJ, USA

Abstract

Integrin signaling impacts many developmental processes. The complexity of these signals increases when multiple, unique integrin heterodimers are expressed during a single developmental event. Since integrin heterodimers have different signaling capabilities, the signals originating at each integrin type must be separated in the cell. *C. elegans* have two integrin heterodimers, α INA-1/β PAT-3 and α PAT-2/β PAT-3, which are expressed individually or simultaneously, based on tissue type. We used chimeric α integrins to assess the role of α integrin cytoplasmic tails during development. Chimeric integrin *ina-1* with the *pat-2* cytoplasmic tail rescued lethality and maintained neuron fasciculation in an *ina-1* mutant. Interestingly, the *pat-2* tail was unable to completely restore distal tip cell migration and vulva morphogenesis. Chimeric integrin *pat-2* with the *ina-1* cytoplasmic tail had a limited ability to rescue a lethal mutation in *pat-2*, with survivors showing aberrant muscle organization, yet normal distal tip cell migration. In a wild type background, α integrin *pat-2* with the *ina-1* cytoplasmic tail had a dominant negative effect which induced muscle disorganization, cell migration defects and lethality. These results show the α integrin cytoplasmic tails impact unique cellular behaviors that vary by tissue type during development.

Keywords

integrin; morphogenesis; distal tip cell; muscle

Introduction

Tissue morphogenesis occurs in the complex and changing environment of a developing organism. Individual cells must interact with and respond to this environment to execute their appropriate developmental fates. One major family of proteins used for communication between the environment and interior of a cell are integrins. Integrins are heterodimeric transmembrane receptors composed of an α and a β subunit. Each subunit has a large extracellular domain, single pass transmembrane region and small cytoplasmic tail (Hynes,

[*]Address correspondence to: Christopher Meighan. Dept. of Molecular Biology and Chemistry, Christopher Newport University, Newport News, VA 23606, USA. Tel: +1-(757) 594-7454. Fax: +1-(757) 594-7356. christopher.meighan@cnu.edu.

2002). Integrins connect the extracellular matrix to cytoplasmic proteins capable of binding and regulating the actin cytoskeleton. These interactions provide both cytoplasmic structure and access to a large number of signaling pathways (Zamir & Geiger, 2001; Lo, 2007). The diversity and importance of integrin signaling is highlighted by its ability to regulate cell division, adhesion, survival, differentiation and migration (Danen & Sonnenberg, 2003; Miranti & Brugge, 2002). Many organisms express multiple integrin types during development. In mice, integrin β1 is capable of forming a heterodimer with 12 different α integrins (Margadant *et al*., 2011). Experiments targeting individual α integrins revealed their dualistic nature as interchangeable or irreplaceable based on tissue type (DeArcangelis & Georges-Labouesse, 2000). For example, despite the expression of six different α integrins that pair with β1 during vasculogenesis, only α5 and α4 have irreplaceable functions (Yang *et al*., 1993; Yang *et al*., 1995; Bouvard *et al*., 2001). On the other hand, α3 is not required during vasculogenesis, but has an irreplaceable role in lung, kidney, brain and skin development (Kreidberg *et al*., 1996; DiPersio *et al*., 1997; Bouvard *et al*., 2001). Multiple integrins can have complementary roles within a single tissue type. For example, neuronal migration in the developing cerebral cortex uses α3 to drive early migratory events and αV to provide extended adhesion (Anton *et al*., 1999; Schmid *et al*., 2004). These examples and many other studies establish the importance of integrins during development and illustrate the complexity in signaling that can result from the simultaneous expression of multiple integrins in single cells. One challenge facing the integrin field is determining the cellular mechanisms used to separate and distinguish signals originating from different integrins in the same cell.

Our work in *C. elegans* established a system of α integrin regulation to control cell migration. In contrast to humans, with 24 different αβ integrin heterodimers, *C. elegans* have only two heterodimers. Loss of α integrin *pat-2* or β integrin *pat-3* causes lethality due to muscle paralysis from a complete disorganization of actin and myosin (Williams & Waterston, 1994; Gettner *et al*., 1995). Nematodes are an excellent system for dissecting integrin activity because the organization of intracellular proteins by the PAT-2/PAT-3 heterodimer in muscle cells has many similarities to focal adhesion complexes in mammals (Cox & Hardin, 2004). Loss of function mutations in the other α integrin, *ina-1*, are lethal due to head morphogenesis defects (Baum & Garriga, 1997). Our previous studies examining distal tip cell (DTC) migration during gonad morphogenesis showed α integrin *ina-1* was required for cell motility while α integrin *pat-2* had a role in pathfinding (Meighan & Schwarzbauer, 2007). The need for two α integrins was striking during the late stage of DTC migration which required both INA-1 and PAT-2 simultaneously for different components of cell migration regulation, suggesting that the signals from each α integrin could be separated in the cell. Here we show, through the use of chimeric integrins, that the α integrins have functional capacities that differ between DTCs, vulval and body wall muscle cells, adding yet another level of complexity and dynamism to integrin signaling during development.

Results

Lethality can be rescued by chimeric integrin transgenes

C. elegans have mirror-image U-shaped gonad arms whose formation depends upon the circuitous migration of the DTCs (Figure 1A) (Hirsh *et al*., 1976). Integrin *ina-1* is expressed during the initial stage of DTC migration on the ventral side (Figure 1A, positions 1–2). During the dorsal stage of DTC migration, both α integrins are expressed simultaneously; *ina-1* activity drives motility while *pat-2* impacts pathfinding (Figure 1A, 3–5) (Meighan & Schwarzbauer, 2007). This finding implies the functional capabilities of each α integrin are separable in the cell and suggests the separation occurs via the cytoplasmic domain. Comparison of the α integrin cytoplasmic domains yield the GFFKR motif, which is highly conserved in mammalian α integrins, and several other similar amino acids (Figure 1B) (Larkin *et al*., 2007; Gahmberg *et al*., 2009). These similarities could allow each α integrin cytoplasmic tail to perform identical functions. In *Drosophila melanogaster*, chimeric integrins of αPS1 and αPS2 with swapped cytoplasmic domains showed the α integrin cytoplasmic tails were interchangeable (Martin-Bermudo *et al*., 1997). To evaluate the importance of the α integrin cytoplasmic tail in signal differentiation during DTC migration, chimeric α integrins were created. The chimeric integrin *ina-1(pat-2cyto)* contains regions encoding the extracellular and transmembrane domains of *ina-1* attached to the cytoplasmic domain of *pat-2* (Figure 1C). The gene construct for *ina-1(pat-2cyto)* is identical to the intact *ina-1* gene, with the exception of the sequence encoding the cytoplasmic domain, and includes the 4 kb *ina-1* promoter region used to drive expression. The chimeric integrin *pat-2(ina-1cyto)* has the extracellular and transmembrane domains of *pat-2* attached to the cytoplasmic domain of *ina-1* (Figure 1C). This gene construct is identical to intact *pat-2* except for the cytoplasmic domain and includes the 6 kb *pat-2* promoter region to drive expression. All constructs used in this study include the gene for the Venus variant of GFP attached via a short linker to the 3′ end of the coding region.

Loss of function mutations in *ina-1* are lethal in larval stage L1 due to the notched head phenotype that results from improper adhesion between epithelial sheets in the head of the nematode (Baum & Garriga, 1997). The ability of chimeric integrin *ina-1(pat-2cyto)* to rescue a lethal allele of *ina-1* was evaluated by injection into strain NG2324, *ina-1(gm86)/qC1 dpy-19(e1259), glp-1(q339)* and compared to rescue by injection of an intact version of *ina-1*. The culmination of multiple rescue events following independent injections showed intact *ina-1* was able to rescue 99.5% of *ina-1(gm86)* homozygotes while *ina-1(pat-2cyto)* was able to rescue 98.4% of *ina-1(gm86)* homozygotes in progeny expressing Venus through the restoration of head morphogenesis (Table 1). The notched head phenotype was only seen in.5% and 1.6% of Venus-expressing progeny rescued with intact *ina-1* or *ina-1(pat-2cyto)* respectively. This rescue of head morphogenesis, and its associated larval lethality, demonstrates the *pat-2* cytoplasmic tail is capable of mimicking *ina-1* cytoplasmic tail activity.

The ability of *pat-2(ina-1cyto)* to rescue normal *pat-2* function was evaluated. Loss of function mutations in *pat-2* are lethal due to paralysis and arrest at the two-fold stage of development (Williams & Waterston, 1994). Evaluation of rescue was performed using

unc-79(e1068), pat-2(st567) homozygotes which showed expression of Venus. When Venus was visible in all embryos, intact *pat-2* resulted in 99.5% (± 0.54) rescue of embryonic lethality. Chimeric *pat-2(ina-1cyto)* had 54% (± 9.2) rescued embryos despite the presence of Venus in all progeny, both rescued and Pat (Table 2). All surviving adults expressed Venus and had uncoordinated movement, the Unc phenotype, as expected in *unc-79(e1068), pat-2(st567)* homozygotes. This showed the *ina-1* cytoplasmic tail was able to substitute for the *pat-2* cytoplasmic tail to rescue lethality. Contrary to intact *pat-2* which rescued the Pat phenotype whenever it was expressed, *pat-2(ina-1cyto)* failed to rescue 46% of the Venus-positive embryos. This result suggests *pat-2(ina-1cyto)* is capable of substituting for *pat-2*, but fails to completely replace *pat-2* cytoplasmic tail function during embryogenesis.

ina-1(pat-2cyto) has defective DTC migration and vulva morphology, yet normal axon fasciculation

Non-lethal mutant *ina-1(gm144)*, which confers a proline to leucine change at position 1072 in the extracellular domain of INA-1 proximal to the transmembrane region, has defects in DTC migration, vulva morphogenesis and nerve fasciculation (Baum & Garriga, 1997). Effects of the *ina-1(pat-2cyto)* chimeric integrin on these developmental processes were analyzed in transgenic nematode lines rescued from lethal allele *ina-1(gm86)*. Lethality in *ina-1(gm86)* nematodes occurs prior to DTC migration, but our work has shown knockdown of *ina-1* by RNAi causes early DTC migration termination, suggesting restored migration in *ina-1(gm86)* homozygotes is driven by the transgene (Meighan & Schwarzbauer, 2007). Since each transgenic line carries an extrachromosomal array, only Venus-positive DTCs were evaluated for proper migration. A small number of DTC migration defects (5.4 ± 1.2%) were present in *ina-1(gm86)* mutants rescued by intact *ina-1*, but the majority had the wild type U-shaped gonad arm indicative of proper DTC migration (Fig. 1A, 2A). In contrast, rescue of *ina-1(gm86)* in three independent lines by *ina-1(pat-2cyto)* averaged 24.8 ± 2.5% DTC migration defects, showing the *pat-2* tail is unable to restore DTC migration to the level achieved by intact *ina-1* (Table 3). The defects included early migration termination (Fig. 2B), extra turns during the dorsal stage of migration (Fig. 2C), and overextension past the vulva (not shown). Venus expression was confirmed in DTCs with aberrant migration (Fig. 2D).

Vulva morphogenesis was also analyzed in transgenic nematodes rescued from lethal allele *ina-1(gm86)*. The mature vulva is located on the ventral surface of the nematode body, but *ina-1(gm86)* causes developmental arrest prior to vulva formation, therefore the impact of each transgene was evaluated only in Venus-positive nematodes (Fig. 1A,3A,B).Analysis of *ina-1(gm86)* rescued with *ina-1(pat-2cyto)* showed protruding vulvas in 43.0% (n=107) of hermaphrodites (Fig. 3D), whereas those rescued by intact *ina-1* had only 3.9% (n=132) protruding vulvas (Fig. 3C). Errors in non-lethal mutant *ina-1(gm144)* appear as protruding vulvas (96% n=114) (Fig. 3E). Unlike *ina-1(gm144)*, in which the vulva often ruptures expelling gonadal and intestinal tissues, *ina-1(pat-2cyto)* rescued animals did not display this phenotype, suggesting that interactions involving this chimeric integrin are better able to maintain tissue integrity than allele *gm144*.

Ina-1 has a well-established role in neuronal function and non-lethal alleles of *ina-1* have defects in bundling axons into fascicules (Baum & Garriga, 1997). If the *ina-1* cytoplasmic tail has a role in axon bundling, we would expect *ina-1(pat-2cyto)* to have errors in ventral cord motor neurons along the length of the body or amphid neurons in the head (Fig. 1A, structures in red). The Venus tag on the integrin allows visualization of the ventral cord motor neurons. These neurons appear as single normal fluorescent fasciculation when intact *ina-1* rescued *ina-1(gm86)* (Fig. 4A). Chimeric *ina-1(pat-2cyto)* rescue of *ina-1(gm86)* yielded identical results as intact *ina-1* (Fig. 4B), with normal fasciculation in 99.1 ±.8% (n=123) and 98.1 ±.8% (n=206) of nematodes for intact *ina-1* and *ina-1(pat-2cyto)* respectively. Similarly, amphid neurons loaded with the vital dye DiI had normal axon fasciculation and normal configuration of the nerve ring and lateral ganglia in both intact *ina-1* and *ina-1(pat-2cyto)* rescued nematodes (Fig. 4C,D). From these experiments, it appears that either the *ina-1* or *pat-2* cytoplasmic tail is sufficient for normal axon bundling. Overall, chimeric *ina-1(pat-2cyto)* is capable of restoring head morphogenesis to rescue lethality and can direct normal axon bundling, yet fails to completely restore DTC migration and vulva morphogenesis. These results indicate that the *ina-1* cytoplasmic tail may have tissue-specific functions.

Dominant negative effects of *pat-2(ina-1cyto)* on DTC migration and body morphology

Chimeric *pat-2(ina-1cyto)* was limited in its ability to rescue *pat-2* mutants as seen by the presence of transgene expression in Pat embryos. The Pat phenotype results from a lack of muscle contraction at the two-fold stage of development; lethality occurs prior to the migration of DTCs and many other developmental events (Williams & Waterston, 1994). The inability of *ina-1(pat-2cyto)* to replicate all *ina-1* functions in late developmental events suggests *pat-2(ina-1cyto)* could be similarly deficient in late developmental events that require *pat-2* function, such as DTC migration guidance (Meighan & Schwarzbauer, 2007). Contrary to our expectations, rescue of the lethal mutant *pat-2(st567)* with an intact *pat-2* or chimeric *pat-2(ina-1cyto)* transgene gave fewer than 10% of survivors with DTC migration defects (Table 3).

Interestingly, introduction of *pat-2(ina-1cyto)* into a wild type background had a dominant negative impact on DTC migration. The *pat-2(ina-1cyto)* transgene generated 19.9 ± 1.0% DTC migration defects compared to 8.0 ± 1.8% for intact *pat-2* (Table 3). Defects included extra turns (Fig. 5A,B) and overextension past the vulva, similar to defects seen when *pat-2* was disrupted by RNAi (Meighan & Schwarzbauer, 2007). This suggests the presence of *pat-2(ina-1cyto)* is able to disrupt normal integrin signaling during DTC migration. With expression of *pat-2(ina-1cyto)* in a wild type background, only 73.9 ± 5.2% (n=780) of progeny reached adulthood. Failure to reach adulthood appeared as larval arrest either as Pat embryos (13.7% of total progeny) or at later larval stages with body morphology defects (Fig. 5C–E) (12.4% of total progeny). Chimeric *pat-2(ina-1cyto)* in a wild type background also had uncoordinated movement in almost all adult nematodes (96.0 ± 2%, n=170). Expression of intact *pat-2* in a wild type background generated no Pat embryos nor early lethality and very few animals with movement defects (3.0±1.8%,n=225). Uncoordinated movement was not evaluated in lines that rescued *pat-2(st567)* due to the closely linked mutation in *unc-79(e1068)*, which generates an uncoordinated phenotype. The ability of the

chimeric integrin to cause embryonic and larval lethality shows *pat-2(ina-1cyto)* has a dominant-negative effect on normal *pat-2* function.

pat-2(ina-1cyto) has disorganized actin filaments in body wall muscle

Due to the inability of *pat-2(ina-1cyto)* to rescue the Pat phenotype in all embryos that expressed the transgene and the body morphology and movement defects in dominant negative *pat-2(ina-1cyto)*, a closer examination of muscle cell function was necessary. *C. elegans* body wall muscle is composed of two major structures: dense bodies and M lines. Dense bodies and M lines organize the actin and myosin filaments in sarcomeres which are required for muscle contraction (MacKenzie *et al*., 1978; Francis & Waterston, 1985). Dense bodies and M lines are anchored at the plasma membrane by the integrin heterodimer PAT-2/PAT-3 (Gettner *et al.*, 1995). Spatial organization of the cytoskeletal components of the sarcomere starts at the membrane and builds inward, meaning a loss of either PAT-2 or PAT-3 results in sarcomere disorganization (Hresko *et al*., 1994; Gettner *et al*., 1995). Alterations in the α integrin cytoplasmic tail could impact the localization of integrins at the membrane or their ability to organize intracellular structures.

Venus-tagged integrin transgenes were localized in the typical dashed pattern in body wall muscle cells of *pat-2* and *pat-2(ina-1cyto)* strains in both rescues of *pat-2(st567)* (Fig. 6A,B) and wild type backgrounds. The lack of obvious integrin disorganization suggests that intracellular abnormalities and not integrin mislocalization are likely to be responsible for errors in muscle function. Muscle structures are easily identified by evaluating actin filament organization. Fixation then staining with rhodamine-phalloidin to view actin filaments revealed several interesting phenotypes. Rescue of *pat-2(st567)* by intact *pat-2* generated actin filament pattern defects in 5.6 ± 1% (n=213) of nematodes; the majority showed normal actin organization (Fig. 6C). In contrast, *pat-2(st567)* rescued by *pat-2(ina-1cyto)* had disorganized actin filaments in 37.3 ± 3.4% (n=210) of nematodes. These defects appeared as gaps or large spaces in the normal pattern of actin staining (Fig. 6D). *pat-2(ina-1cyto)* in a wild type background had disorganized actin in 62 ± 2.7% (n=235) of nematodes (Fig. 6E), a significant increase compared to the minimal disorganization (1.1 ± 1%, n=147) in wild type lines expressing the intact *pat-2* transgene. When *pat-2(ina-1cyto)* in a wild type background showed body morphology defects, almost no distinct actin filaments could be seen and rhodamine-phalloidin staining lacked the uniformity and linear organization observed in normal muscle (Fig. 6F). These abnormalities were not detected in N2 nematodes or strains transgenic for a transcriptional fusion of the *pat-2* promoter to GFP (not shown). The presence of actin disorganization by the dominant negative *pat-2*(*ina-1cyto)* shows the *ina-1* cytoplasmic tail can disrupt intracellular processes in muscle cells consistent with observed movement defects. The ina-1 cytoplasmic tail is either deficient in recruiting the appropriate actin modifiers to dense bodies or preventing the usual dense body components from functioning properly.

Discussion

Our earlier work using *C. elegans* to study integrin-directed cell migration revealed both α integrins *ina-1* and *pat-2* were used simultaneously to direct different aspects of the distal tip

cell migratory process. Here we show, using chimeric α integrins, that α integrin cytoplasmic tails are not functionally interchangeable. While both chimeric integrins were able to rescue lethality, rescued nematodes had tissue-specific defects.*Ina-1* mutants rescued with *ina-1(pat-2cyto)* had defects in DTC migration and vulva morphogenesis showing that the *pat-2* cytoplasmic tail cannot fully replicate *ina-1* activities. On the other hand, rescue of a *pat-2* mutant with *pat-2(ina-1cyto)* gave normal DTC migration but abnormal muscle organization. This chimeric integrin also caused dominant negative muscle defects in a wild type background. Together, our results indicate the *ina-1* and *pat-2* cytoplasmic tails have tissue-specific roles in α integrin function.

The tissue-specific present in transgenic nematodes provide an interesting contrast to the αPS1 and αPS2 integrins in *Drosophila melanogaster*. Lethality of αPS1 or αPS2 could be rescued by expression of the other α integrin or a chimeric version with the opposite cytoplasmic tail in *D. melanogaster*, just as the chimeric integrins successfully rescued lethality in nematodes (Martin-Bermudo *et al*.,1997). As further evidence of the interchangeability of α integrin cytoplasmic tails, recruitment of intracellular protein tensin could be accomplished by either intact αPS2 or chimeric αPS2 with an αPS1 cytoplasmic tail (Delon and Brown, 2009). While both organisms allow interchangeability of the cytoplasmic tails to rescue lethality, chimeric integrins in *D. melanogaster* do not appear to generate tissue-specific defects. This difference suggests α integrin function in lower organisms is not universal.

The observed defects in DTC migration, vulva morphogenesis, and muscle function with rescue of lethality by chimeric integrins could be explained by alterations in extracellular matrix binding or by changes in cytoplasmic interactions with signaling/cytoskeletal partners. However, the ability of *pat-2(ina-1cyto)* to generate dominant negative effects in muscle supports the second explanation, i.e., that the *ina-1* cytoplasmic tail is directly responsible for the abnormalities, since muscle cell adhesion is maintained by endogenousPAT-2/PAT-3. Furthermore, adult survivors rescued by PAT-2(INA-1cyto) showed proper localization of the transgene product in body wall muscle which supports the idea that the chimeric integrin is able to bind to its extracellular matrix ligand. Talin, vinculin, α-actinin, integrin-linked kinase and many other cytoplasmic proteins are required for dense body and M line formation and function in muscle cells (Francis & Waterston, 1985; Barstead & Waterston, 1991;Barstead *et al*.,1991;Moulder *et al*.,1996;Mackinnon *et al*., 2002). The *ina-1* cytoplasmic tail could be altering the recruitment or use of any or all of these sarcomere proteins. The close relationship between mammalian focal adhesions and dense bodies in *C. elegans* suggests the mechanisms used by the *pat-2* cytoplasmic tail to organize muscle structure could be conserved in higher organisms (Cox and Hardin, 2004).

There are precedents for α integrin-directed intracellular signaling. Amino acid sequence homology between either INA-1 or PAT-2 and the mammalian α integrin cytoplasmic tails suggests a general similarity in length, in the presence of the GFFKR motif, and in multiple phosphorylatable tyrosine, serine and threonine residues (Gahmberg *et al*., 2009). Mammalian integrins have been shown to have tail-specific binding partners. For instance, the α4 cytoplasmic tail directly binds cytoplasmic structural and signaling protein paxillin (Liu *et al*., 1999). Cyclic changes in the phosphorylation state of the α4 tail regulated

paxillin binding, meaning the interaction of the α tail with cytoplasmic proteins is dynamic and regulated (Liu & Ginsberg, 2000; Han *et al.*, 2003). Disruption of paxillin binding to α4 can impact talin function and reduce cell adhesion, showing the activity present at the α integrin can also impact proteins associated with β integrin function (Alon *et al*., 2005). Paxillin and talin are both present in *C. elegans* and could contribute to all three phenotypes impacted by the chimeric integrins. Sequence motif GFFKR is present in both INA-1 and PAT-2; this motif has been implicated in binding mammalian Bin1, Mss4 and Nischarin (O'Toole *et al*., 1994; Wixler *et al*., 1999; Alahari *et al*., 2000). The α5 cytoplasmic tail has been shown to bind to the tight junction protein zonula occludens-1 providing directionality to migrating tumor cells (Tuomi *et al*., 2009). Overall, these studies provide evidence that α tails have important roles in cell behavior modification. The inability of the *pat-2* cytoplasmic tail to substitute for the *ina-1* cytoplasmic tail in the DTCs and vulva suggests the *ina-1* tail can influence unique signaling partners that are either inaccessible or simply recruited at a lower affinity by*pat-2*. This is further supported by the dominant negative activity seen with *pat-2(ina-1cyto)*; where the disruption in normal *pat-2* function could be explained by *pat-2(ina-1cyto)* recruiting inappropriate signaling partners or blocking normal *pat-2* function. Conversely, the ability of the *pat-2* cytoplasmic tail to rescue *ina-1* mutant lethality suggests other α integrin functions can be executed by either tail, perhaps by accessing the same signaling pathways or by alternative mechanisms that are α tail independent. If each cytoplasmic tail has multiple unique binding partners, signals originating at distinct integrin types could be differentiated by modifying the signaling partners present in different cell types or over time in the same cell type.

Of course, it is also possible that swapping the integrin tails changes the ability to recognize extracellular matrix binding sites. INA-1/PAT-3 is predicted to bind laminin while PAT-2/PAT-3 is predicted to bind RGD amino acid motifs (Brown, 2000). Neither of these interactions has been demonstrated experimentally in *C. elegans* so it is not possible to directly test chimeric integrin binding to the matrix. Thus it remains possible that chimeric integrins have altered ligand binding activity. However, if altered affinity is the sole factor in generating the phenotypes present in the chimeric lines, then the tissues that typically lead to lethality in α integrin mutants, muscle and head morphogenesis, can develop normally with altered ligand binding. Logically, these tissues should be the most sensitive to changes in integrin binding strength. Clearly, the verification of integrin extracellular binding partners, their distribution and use throughout nematode development remains a large and important component in understanding integrin function.

In conclusion, the cytoplasmic tails of α integrins *ina-1* and *pat-2* make tissue-specific contributions to integrin signaling. Determining the mechanisms used by the cytoplasmic tails to impact signaling could include alterations in extracellular ligand binding affinity or changes in intracellular signaling partners. The varied use of α integrin cytoplasmic tails in different cell types and developmental events in a single organism further demonstrates the flexibility and complexity of integrins, highlighting their position as central molecules in cell behavior.

Materials and Methods

Strains and genetics

Nematodes were maintained at 23 degrees following standard protocols (Brenner, 1974). N2 was used as wild type. Mutant strains used were NG144, *ina-1(gm144)*; NG2324, *ina-1(gm86)/qC1 dpy-19(e1259), glp-1(q339)*; and RW1536, *unc-79(e1068), pat-2(st567)/ dpy-17(e164)*.

Strain construction

Intact *ina-1* and *ina-1(pat-2cyto)*—Strain *ina-1(gm86); Ex[ina-1p::ina-1::venus, rol-6(su1006)]*, referred to as intact *ina-1*, and strain *ina-1(gm86); Ex[ina-1p::ina-1/ pat-2cyto::venus, rol-6(su1006)]*, referred to as *ina-1(pat-2cyto)*, were constructed via multiple PCR and restriction digestion reactions. Plasmid pHSina1cDNA contains the complete *ina-1* cDNA, except the stop codon has been replaced with an AgeI restriction site. To add Venus, primers VenusIna1F and p95R were used to amplify a cassette containing the Venus variant of GFP attached to the *unc-54* 3′ UTR from p95.79-wVenus, Addgene plasmd 37466 (Yamamoto *et al*., 2011). VenusIna1F created a linker sequence encoding Pro Val Ala Lys between the end of the *ina-1* coding sequence and the start of Venus. The same linker was used for all *ina-1* cytoplasmic tail Venus constructs. An AgeI and SpeI digest was used to clone the linker sequence-Venus cassette into the complete *ina-1* cDNA in pHSina1cDNA to create pHSina1cDNA-v. 4.3 kb of *ina-1* promoter was cloned by PCR from genomic DNA using primers ina1pFBamHI and Ina1PkpnIR and inserted upstream of the *ina-1* cDNA.

Replacement of the *ina-1* cytoplasmic tail with the *pat-2* cytoplasmic tail occurred prior to the Venus and promoter additions. The terminal 972 bp of *ina-1* cDNA were amplified from the plasmid pHSina-1cDNA by PCR using primers ina1CyBamHIF and ina1CyBamHIR, then subcloned into the BamHI site of pSP73, creating pSP73ina1c. The *pat-2* cytoplasmic tail was amplified from pHSpat-2cDNA using primers pat2FPsiI and pat2RAgeI, digested with PsiI and AgeI then cloned in place of the *ina-1* cytoplasmic tail in pSP73ina1c. A digest with BglII and AgeI was used to clone *ina-1* with the *pat-2* cytoplasmic tail into the complete *ina-1* cDNA present in pHSina1cDNA. Venus and the *ina-1* promoter were added as described above, except primer VenusPat2F was used in place of VenusIna1F.

Intact *pat-2* and *pat-2(ina-1cyto)*—Strain *unc-79(e1068), pat-2(st567); Ex[pat-2p::pat-2::venus, rol-6(su1006)]*, referred to as intact *pat-2*, and strain *unc-79(e1068), pat-2(st567); Ex[pat-2p::pat-2/ina-1cyto::venus, rol-6(su1006)]*, referred to as *pat-2(ina-1cyto)*, were constructed through a combination of fusion PCR and restriction digests. Fusion PCR to construct intact *pat-2* connected the *pat-2* cytoplasmic tail to the Venus variant of GFP (Hobert, 2002). Plasmid pKAG contains the entire *pat-2* gene, including 6 kb of upstream promoter (Meighan & Schwarzbauer, 2007). The terminal 2.8 kb of *pat-2* was amplified from position +4198, where the A in ATG is +1, to the penultimate codon with primers pat2FA1 and pat2BR. Primer pat2BR matches the 3′ end of the *pat-2* gene, contains the linker sequence followed by a small portion of the Venus gene. The linker sequence encoding Thr Gly Ala Lys between the end of the *pat-2* coding sequence and the

start of Venus is identical in all pat-2 cytoplasmic tail constructs used in this project. Plasmid p95.79wVenus was used to amplify Venus and the *unc-54* 3′ UTR with primers VenusPat2F and VenusPat2R1. The products from both reactions were used as templates for fusion PCR using primers Pat2FA2 and Venus-Pat2R2. The new PCR product spanning from +5385 of the *pat-2* gene to the end of the 3′ UTR was inserted at the BglII site at position +5385 in the original plasmid containing 6kb of *pat-2* promoter and the *pat-2* gene. Prior to insertion, a BglII site at position −3439 was removed from the plasmid by digest with SacI. After insertion at the BglII site at position +5385, the section of the promoter removed by SacI was replaced.

Construction of *pat-2(ina-1cyto)* used fusion PCR to replace the *pat-2* cytoplasmic tail with the *ina-1* cytoplasmic tail. The *pat-2* gene was amplified by primer pat2FA1 at position +4198 with reverse primer pat2ina1R, a primer that connects the transmembrane domain of *pat-2* with an overhang matching the cytoplasmic tail of *ina-1*. Plasmid pHSina1cDNA-v was used to amplify the *ina-1* transmembrane region, *ina-1* cytoplasmic domain, Venus and the 3′UTR of *unc-54* using primers ina1TMF and VenusPat2R1. Both products were used as a template for fusion PCR with primers pat2FA2 and VenusPat2R2 followed by insertion at the BglII site at position +5385 as described above.

PCR-generated sections were verified by sequence analysis. Constructs were injected at 30 μg/ml of construct with 100 μg/ml of pRF4 *rol-6(su1006)* into strain NG2324 for the *ina-1* constructs and strain RW1536 for *pat-2* constructs. At least three independent injection events were used to create lines for each construct. Lines used for analysis had stable expression patterns comparable to promoter fusions to GFP or RFP for *ina-1* or *pat-2* (Meighan & Schwarzbauer, 2007).

Scoring and rescue calculations

Strain NG2324, *ina-1(gm86)/qC1 dpy-19(e1259), glp-1(q339),* generates 25% lethality at L1 due to *ina-1(gm86).* Rescue of this line by a transgene reduces the percentage of dead notched head L1 nematodes. To calculate percent rescue for *ina-1(gm86)/ina-1(gm86),* the number of L1 lethal nematodes was subtracted from the total progeny then divided by the total progeny, similar to Martin-Bermudo *et al.*, (1997). Only Venus-positive nematodes were evaluated.

Strain RW1536, *unc-79(e1068), pat-2(st567)/dpy-17(e164),* generates 25% lethality at the two-fold stage of development. A *pat-2* rescue in these nematodes is expected to reduce the number of Pat embryos while creating the Unc phenotype in rescued adults due to the *unc-79(e1068)* allele. To calculate percent rescue for *unc-79(e1068), pat-2(st567)/ unc-79(e1068), pat-2(st567),* the number of Pat embryos was subtracted from the total progeny then divided by the total progeny, similar to Martin-Bermudo *et al.*, (1997). Only Venus-positive nematodes were evaluated.

Quantification of abnormal movement was achieved by stimulating nematodes with multiple eyelash touches followed by counting seconds of movement. Movement for 1 second or less was considered uncoordinated.

DTC migration defects were categorized by DTC position in adult nematodes. Migration was scored as early termination if the DTC was 3 or more egg lengths short of the vulva; overextension if the DTC migrated 3 or more egg lengths past the vulva; extra turns if the DTC made any turns outside those seen in wild type migration. Only Venus-positive nematodes were evaluated.

Staining and microscopy

Actin organization in *pat-2* lines was evaluated with Rhodamine-conjugated phalloidin (Molecular Probes). Fixation and staining protocols were followed as previously described (Lee *et al*., 2001; Cram *et al*., 2003). Briefly, nematodes were fixed in methanol and acetone then stained with rhodamine-conjugated phalloidin for 2 hours at room temperature.

Amphid neurons fasciculation was evaluated by loading with 1,1′-Diocta-decyl-3,3,3′,3′-Tetramethylindocarbocyanine Perchlorate (DiI) following the protocol described by Hedgecock *et al.,* (1985), except FITC was replaced with DiI. Briefly, 50ul of 20mg/ml DiI in ethanol was added to seeded agar plates and allowed to dry. Adult nematodes were placed on DiI-containing plates for 2 hours then moved to a fresh, non-DiI containing plate for 10 minutes prior to viewing.

A Nikon Eclipse TE 2000U microscope equipped for epifluorescence with a Cooke SensiCam High-Performance camera and IPLab software (Scanalytics) was used to generate fluorescent and DIC images. Nematodes were mounted for microscopy using 60mM sodium azide in M9.

Calculations

Averages and standard error throughout the paper were calculated using the results from multiple independent lines analyzed in at least three different experiments. P values were generated using a Student's Ttest.

Primer List

ina1CyBamHIF	GGGATCCAGGCAGAGCTGGAGATCT
ina1CyBamHIR	GGGATCCACCGGTAGTCCCGTATCA
ina1TMF	ACATCTGCTGATCCTGATAG
ina1pFBamHI	TTGGATCCTTTGTTGTCTATTCAGATGGT
Ina1PkpnIR	TTCGGTACCCGTTTGCCCAGACTC
p95R	CCAAAAAGCAAAAGCAG
pat2BR	ACTCATTTTTGCTACCGGTACTAGCATTTGTCCGTGACGTCC
pat2FA1	TCTAGACATTACTTTAAAGGTACA
pat2FA2	CTTGCCACGATCTCATAGTCGTTG
pat2FPsiI	GCGTTATAATTTGTCTCTGGAGGTGTGGTTTC
pat2ina1R	TCGTTTGAAGAAACCACATTTTGAGAGCAGTAAAATAAGAAGAAT
pat2RAgeI	AACCGGTTAGCATTTGTCCGTGACG
VenusIna1F	GTACCGGTAGCAAAAATGAGTAAAG
VenusPat2F	GGACCGGTGCAAAAATGAGTAAAGG
VenusPat2R1	TCAAATTATCAACTTCTACTC

VenusPat2R2 AAGATCTCCAAAAAGCAAAAGCAGGAA

Acknowledgments

This work was supported by NIH R01 GM059383 (to JES) and by a CNU faculty development grant (to CMM). We would like to thank Hongyu Shang, Hitoshi Sawa and the Caenorhabditis Genetics Center, which is funded by the NIH National Center for Research Resources, for strains provided.

Abbreviations used in this paper

DTC distal tip cell

References

ALAHARI SK, LEE JW, JULIANO RL. Nischarin, a novel protein that interacts with the integrin alpha5 subunit and inhibits cell migration. J Cell Biol. 2000; 151:1141–1154. [PubMed: 11121431]

ALON R, FEIGELSON SW, MANEVICH E, ROSE DM, SCHMITZ J, OVERBY DR, WINTER E, GRABOVSKY V, SHINDER V, MATTHEWS BD, SOKOLOVSKY-EISENBERG M, INGBER DE, BENOIT M, GINSBERG MH. Alpha4beta1 dependent adhesion strengthening under mechanical strain is regulated by paxillin association with the alpha4-cytoplasmic domain. J Cell Biol. 2005; 171:1073–1084. [PubMed: 16365170]

ANTON ES, KREIDBERG JA, RAKIC P. Distinct functions of alpha3 and alpha(v) integrin receptors in neuronal migration and laminar organization of the cerebral cortex. Neuron. 1999; 22:277–289. [PubMed: 10069334]

BARSTEAD RJ, KLEIMAN L, WATERSTON RH. Cloning, sequencing, and mapping of an alpha-actinin gene from the nematode Caenorhabditis elegans. Cell Motil Cytoskeleton. 1991; 20:69–78. [PubMed: 1756579]

BARSTEAD RJ, WATERSTON RH. Vinculin is essential for muscle function in the nematode. J Cell Biol. 1991; 114:715–724. [PubMed: 1907975]

BAUM PD, GARRIGA G. Neuronal migrations and axon fasciculation are disrupted in ina-1 integrin mutants. Neuron. 1997; 19:51–62. [PubMed: 9247263]

BOUVARD D, BRAKEBUSCH C, GUSTAFSSON E, ASZÓDI A, BENGTSSON T, BERNA A, FÄSSLER R. Functional consequences of integrin gene mutations in mice. Circ Res. 2001; 89:211–223. [PubMed: 11485971]

BRENNER S. The genetics of Caenorhabditis elegans. Genetics. 1974; 77:71–94. [PubMed: 4366476]

BROWN NH. Cell-cell adhesion via the ECM: integrin genetics in fly and worm. Matrix Biol. 2000; 19:191–201. [PubMed: 10936444]

COX EA, HARDIN J. Sticky worms: adhesion complexes in C. elegans. J Cell Sci. 2004; 117:1885–1897. [PubMed: 15090594]

CRAM EJ, CLARK SG, SCHWARZBAUER JE. Talin loss-of-function uncovers roles in cell contractility and migration in C. elegans. J Cell Sci. 2003; 116:3871–3878. [PubMed: 12915588]

DANEN EH, SONNENBERG A. Integrins in regulation of tissue development and function. J Pathol. 2003; 201:632–641. [PubMed: 14648669]

DEARCANGELIS A, GEORGES-LABOUESSE E. Integrin and ECM functions: roles in vertebrate development. Trends Genet. 2000; 16:389–395. [PubMed: 10973067]

DELON I, BROWN NH. The integrin adhesion complex changes its composition and function during morphogenesis of an epithelium. J Cell Sci. 2009; 122:4363–4374. [PubMed: 19903692]

DIPERSIO CM, HODIVALA-DILKE KM, JAENISCH R, KREIDBERG JA, HYNES RO. alpha3beta1 Integrin is required for normal development of the epidermal basement membrane. J Cell Biol. 1997; 137:729–742. [PubMed: 9151677]

FRANCIS GR, WATERSTON RH. Muscle organization in Caenorhabditis elegans: localization of proteins implicated in thin filament attachment and I-band organization. J Cell Biol. 1985; 101:1532–1549. [PubMed: 2413045]

GAHMBERG CG, FAGERHOLM SC, NURMI SM, CHAVAKIS T, MARCHESAN S, GRÖNHOLM M. Regulation of integrin activity and signalling. Biochim Biophys Acta. 2009; 1790:431–444. [PubMed: 19289150]

GETTNER SN, KENYON C, REICHARDT LF. Characterization of beta pat-3 heterodimers, a family of essential integrin receptors in C. elegans. J Cell Biol. 1995; 129:1127–1141. [PubMed: 7744961]

HAN J, ROSE DM, WOODSIDE DG, GOLDFINGER LE, GINSBERG MH. Integrin alpha 4 beta 1-dependent T cell migration requires both phosphorylation and dephosphorylation of the alpha 4 cytoplasmic domain to regulate the reversible binding of paxillin. J Biol Chem. 2003; 278:34845–34853. [PubMed: 12837751]

HEDGECOCK EM, CULOTTI JG, THOMSON JN, PERKINS LA. Axonal guidance mutants of Caenorhabditis elegans identified by filling sensory neurons with fluorescein dyes. Dev Biol. 1985; 111:158–170. [PubMed: 3928418]

HIRSH D, OPPENHEIM D, KLASS M. Development of the reproductive system of Caenorhabditis elegans. Dev Biol. 1976; 49:200–219. [PubMed: 943344]

HOBERT O. PCR fusion-based approach to create reporter gene constructs for expression analysis in transgenic C. elegans. Biotechniques. 2002; 32:728–730. [PubMed: 11962590]

HRESKO MC, WILLIAMS BD, WATERSTON RH. Assembly of body wall muscle and muscle cell attachment structures in Caenorhabditis elegans. J Cell Biol. 1994; 124:491–506. [PubMed: 8106548]

HYNES RO. Integrins: bidirectional, allosteric signaling machines. Cell. 2002; 110:673–687. [PubMed: 12297042]

KREIDBERG JA, DONOVAN MJ, GOLDSTEIN SL, RENNKE H, SHEPHERD K, JONES RC, JAENISCH R. Alpha 3 beta 1 integrin has a crucial role in kidney and lung organogenesis. Development. 1996; 122:3537–3547. [PubMed: 8951069]

LARKIN MA, BLACKSHIELDS G, BROWN NP, CHENNA R, MCGETTIGAN PA, MCWILLIAM H, VALENTIN F, WALLACE IM, WILM A, LOPEZ R, THOMPSON JD, GIBSON TJ, HIGGINS DG. Clustal W and Clusat X version 2.0. Bioinformatics. 2007; 23:2947–2948. [PubMed: 17846036]

LEE M, CRAM EJ, SHEN B, SCHWARZBAUER JE. Roles for beta(pat-3) integrins in development and function of Caenorhabditis elegans muscles and gonads. J Biol Chem. 2001; 276:36404–36410. [PubMed: 11473126]

LIU S, THOMAS SM, WOODSIDE DG, ROSE DM, KIOSSES WB, PFAFF M, GINSBERG MH. Binding of paxillin to alpha4 integrins modifies integrin-dependent biological responses. Nature. 1999; 402:676–681. [PubMed: 10604475]

LIU S, GINSBERG MH. Paxillin binding to a conserved sequence motif in the alpha 4 integrin cytoplasmic domain. J Biol Chem. 2000; 275:22736–22742. [PubMed: 10781578]

LO SH. Focal adhesions: what's new inside. Dev Biol. 2006; 294:280–91. [PubMed: 16650401]

MACKENZIE JM JR, GARCEA RL, ZENGEL JM, EPSTEIN HF. Muscle development in Caenorhabditis elegans: mutants exhibiting retarded sarcomere construction. Cell. 1978; 15:751–762. [PubMed: 728988]

MACKINNON AC, QADOTA H, NORMAN KR, MOERMAN DG, WILLIAMS BD. C. elegans PAT-4/ILK functions as an adaptor protein within integrin adhesion complexes. Curr Biol. 2002; 12:787–797. [PubMed: 12015115]

MARGADANT C, MONSUUR HN, NORMAN JC, SONNENBERG A. Mechanisms of integrin activation and trafficking. Curr Opin Cell Biol. 2011; 23:607–614. [PubMed: 21924601]

MARTIN-BERMUDO MD, DUNIN-BORKOWSKI OM, BROWN NH. Specificity of PS integrin function during embryogenesis resides in the alpha subunit extracellular domain. EMBO J. 1997; 16:4184–4193. [PubMed: 9250662]

MEIGHAN CM, SCHWARZBAUER JE. Control of C. elegans hermaphrodite gonad size and shape by vab-3/Pax6-mediated regulation of integrin receptors. Genes Dev. 2007; 21:1615–1620. [PubMed: 17606640]

MIRANTI CK, BRUGGE JS. Sensing the environment: a historical perspective on integrin signal transduction. Nat Cell Biol. 2002; 4:E83–90. [PubMed: 11944041]

MOULDER GL, HUANG MM, WATERSTON RH, BARSTEAD RJ. Talin requires beta-integrin, but not vinculin, for its assembly into focal adhesion-like structures in the nematode Caenorhabditis elegans. Mol Biol Cell. 1996; 7:1181–1193. [PubMed: 8856663]

O'TOOLE TE, KATAGIRI Y, FAULL RJ, PETER K, TAMURA R, QUARANTA V, LOFTUS JC, SHATTIL SJ, GINSBERG MH. Integrin cytoplasmic domains mediate inside-out signal transduction. J Cell Biol. 1994; 124:1047–1059. [PubMed: 7510712]

SCHMID RS, SHELTON S, STANCO A, YOKOTA Y, KREIDBERG JA, ANTON ES. alpha3beta1 integrin modulates neuronal migration and placement during early stages of cerebral cortical development. Development. 2004; 131:6023–6031. [PubMed: 15537685]

TUOMI S, MAI A, NEVO J, LAINE JO, VILKKI V, OHMAN TJ, GAHMBERG CG, PARKER PJ, IVASKA J. PKCepsilon regulation of an alpha5 integrin-ZO-1 complex controls lamellae formation in migrating cancer cells. Sci Signal. 2009; 2:ra32. [PubMed: 19567915]

WILLIAMS BD, WATERSTON RH. Genes critical for muscle development and function in Caenorhabditis elegans identified through lethal mutations. J Cell Biol. 1994; 124:475–90. [PubMed: 8106547]

WIXLER V, LAPLANTINE E, GEERTS D, SONNENBERG A, PETERSOHN D, ECKES B, PAULSSON M, AUMAILLEY M. Identification of novel interaction partners for the conserved membrane proximal region of alpha-integrin cytoplasmic domains. FEBS Lett. 1999; 445:351–355. [PubMed: 10094488]

YAMAMOTO Y, TAKESHITA H, SAWA H. Multiple Wnts redundantly control polarity orientation in Caenorhabditis elegans epithelial stem cells. PLoS Genet. 2011; 7:e1002308. [PubMed: 22022276]

YANG JT, RAYBURN H, HYNES RO. Embryonic mesodermal defects in alpha 5 integrin-deficient mice. Development. 1993; 119:1093–1105. [PubMed: 7508365]

YANG JT, RAYBURN H, HYNES RO. Cell adhesion events mediated by alpha 4 integrins are essential in placental and cardiac development. Development. 1995; 121:549–560. [PubMed: 7539359]

ZAMIR E, GEIGER B. Components of cell-matrix adhesions. J Cell Sci. 2001; 114:3577–3579. [PubMed: 11707509]

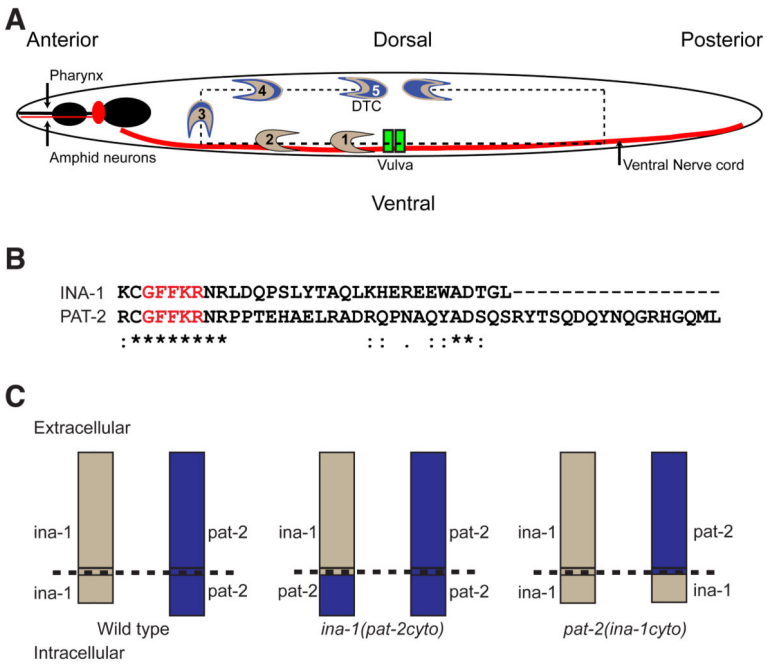

Fig. 1. Models of *α* integrin expression and chimeric integrin structure

(A) α integrin expression during DTC migration. The DTC (crescent) begins migration at the gonad primordium (1), proceeds along the ventral surface (2), then turns and migrates to the dorsal surface (3). Migration continues on the dorsal surface (4) toward the center of the nematode body where migration ends (5). A dashed line represents the path of DTC migration, a solid line is the ventral surface of the nematode body. Tan represents *ina-1* expression, blue represents *pat-2* expression. The vulva, pharynx, amphid neurons and ventral nerve cord are labeled. **(B)** Clustal alignment of INA-1 and PAT-2 cytoplasmic tails. * indicates a fully conserved residue,: indicates a strong group is conserved,. indicates a weak group is conserved. Text in red indicates conserved GFFKR motif. **(C)** Model of chimeric integrins. Extracellular, transmembrane and cytoplasmic domains of *ina-1* and *pat-2* are represented by tan and blue rectangles respectively. The interior and exterior of the cell is indicated with the plasma membrane shown as a dashed line. For chimeric integrin *ina-1(pat-2cyto)*, the extracellular and transmembrane domain of *ina-1* is attached to the cytoplasmic domain of *pat-2*. For chimeric integrin *pat-2(ina-1cyto)*, the extracellular and transmembrane domain of *pat-2* is attached to the cytoplasmic domain of *ina-1*.

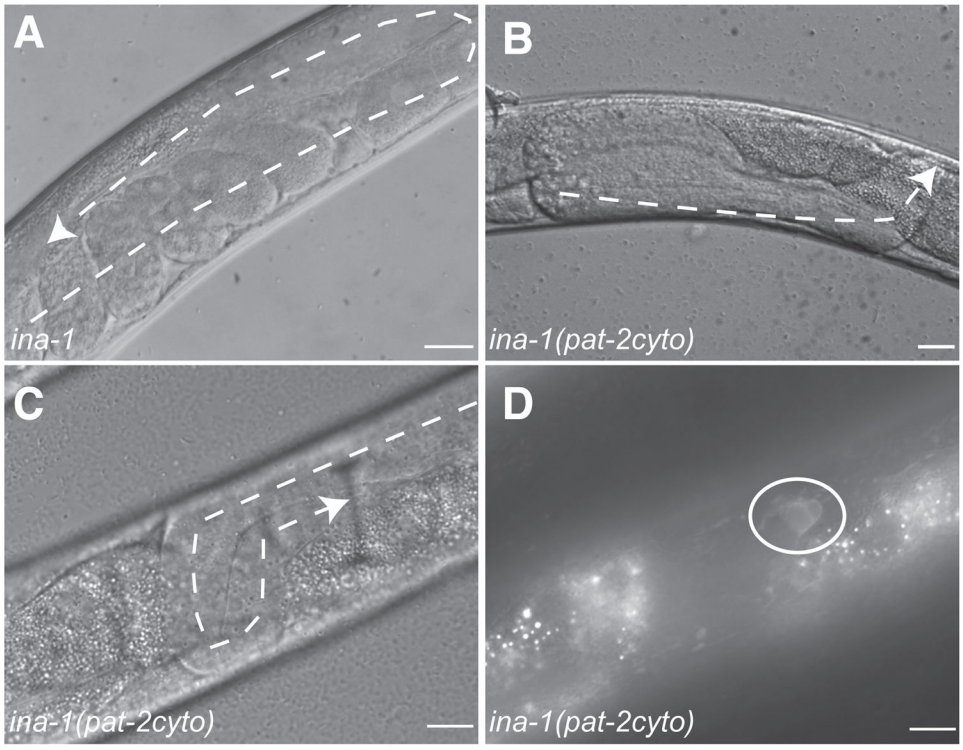

Fig. 2. Chimeric integrin *ina-1(pat-2cyto)* causes distal tip cell (DTC) migration defects

(A) *ina-1(gm86)* nematodes rescued by intact *ina-1* have normal DTC migration. Rescue by *ina-1(pat-2cyto)* gave DTC migration defects including early cessation of migration **(B)** and improper turns **(C). (D)** Expression of Venus in the DTC (white circle) from the rescue by *ina-1(pat-2cyto)* shown in **C**. White lines trace the migratory path of the gonad arms, arrowheads mark the DTCs. Anterior is to the left, dorsal to the top. Scale bar, 25 μm.

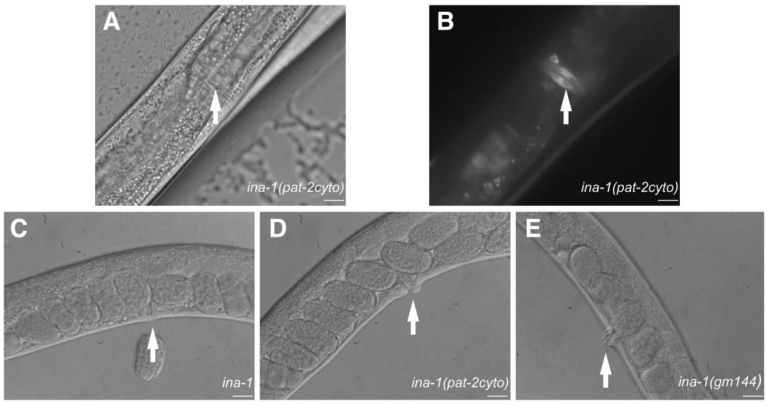

Fig. 3. Chimeric integrin *ina-1(pat-2cyto)* causes vulva morphogenesis defects

Ventral view of brightfield **(A)** and Venus expression **(B)** in the vulval epithelium of *ina-1(pat-2cyto)* nematodes. Loss of function *ina-1(gm86)* nematodes rescued by intact *ina-1* **(C)** have normal vulva morphogenesis. Rescue by *ina-1(pat-2cyto)* has vulva morphogenesis defects **(D)** that appear similar morphologically to *ina-1(gm144)* **(E)**. Arrows point to the vulva. Scale bar, 25 μm.

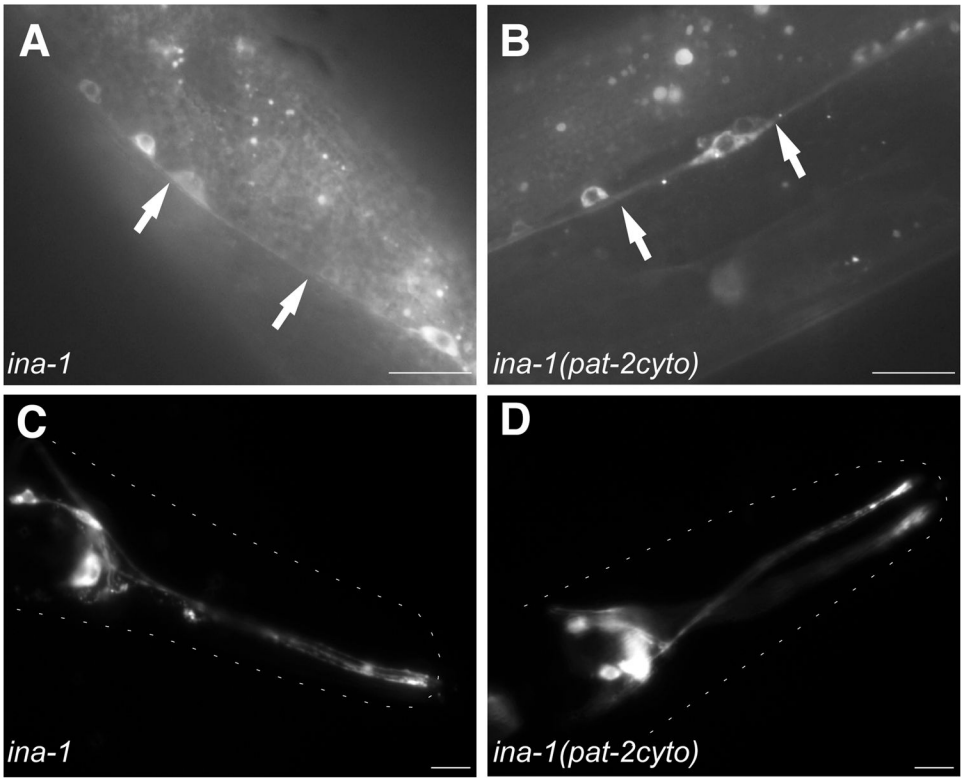

Fig. 4. Neuron fasciculation with wild type and chimeric integrins

Intact *ina-1* **(A,C)** or chimeric *ina-1(pat-2cyto)* **(B,D)** gene constructs were used to rescue loss of function mutation *ina-1(gm86)*. Arrows point to the ventral nerve cord processes along the mid-body, see Figure 1A **(A,B)**. Amphid neuron organization in the pharyngeal nerve ring was visualized by DiI dye loading **(C,D)**. Dashed line traces the head. Anterior is to the right. Scale bar, 25um.

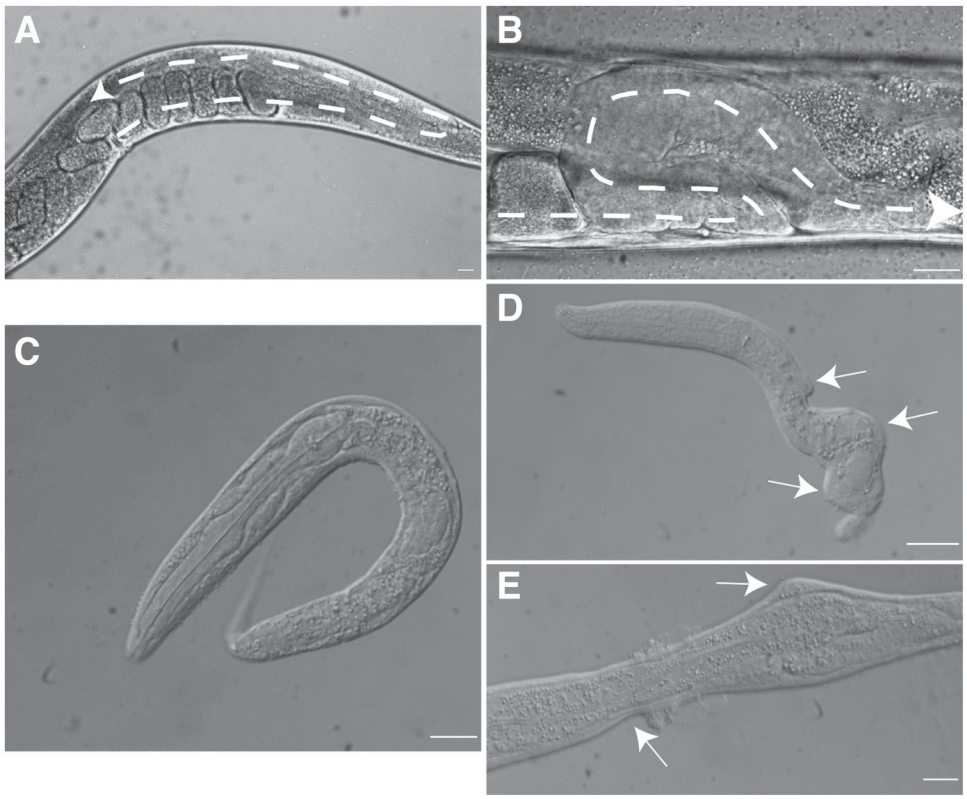

Fig. 5. Dominant negative effects of *pat-2(ina-1cyto)* on distal tip cell (DTC) migration and body morphology

(A) N2 nematode with wild type DTC migration. **(B)** Chimeric *pat-2(ina-1cyto)* causes DTC migration defects in a wild type background. Dashed line overlays the gonad arms, arrowhead is on the DTC. *pat-2(ina-1cyto)* in a wild type background at larval stage L1 with normal body patterning **(C)** and post-hatching body morphology defects in L1 **(D)** and L2 **(E)** nematodes. Arrows point to misshapen structures. Scale bar, 25 μm. Note scale bar changes to indicate changes in nematode size.

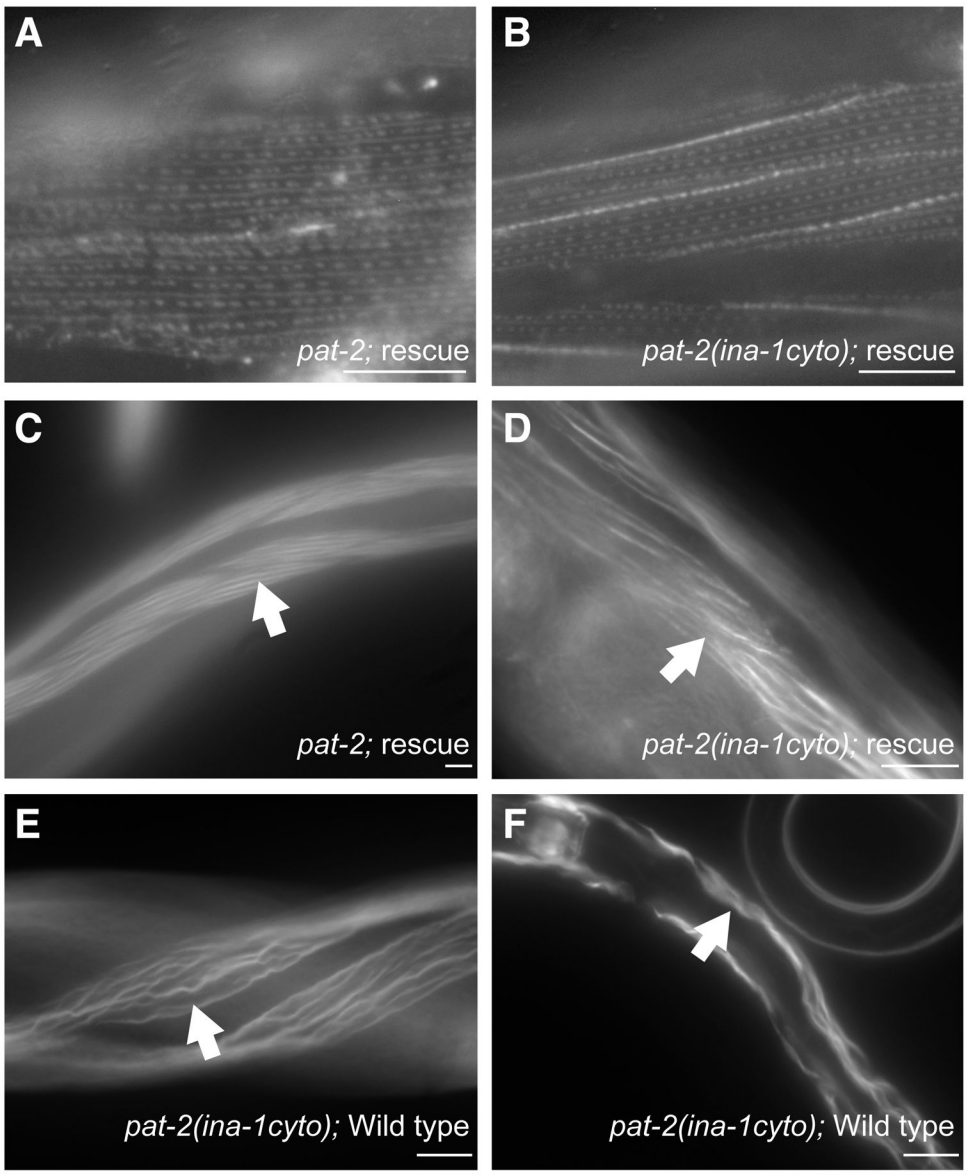

Fig. 6. *pat-2(ina-1cyto)* fails to properly organize body wall muscle actin filaments

Intact PAT-2 **(A)** and chimeric PAT-2(INA-1cyto) **(B)** are localized in the typical dashed line pattern associated with muscle sarcomeres on a *pat-2(st567)* mutant background. **(C)** Actin filaments viewed by rhodamine-phalloidin staining are organized in intact *pat-2* rescue lines of *pat-2(st567)*. Actin filaments are disorganized in *pat-2(ina-1cyto)* rescue lines of *pat-2(st567)* **(D)** as well as when *pat-2(ina-1cyto)* is expressed in a wild type background **(E). (F)** Larval nematode with actin disorganization when *pat-2(ina-1cyto)* is expressed in a wild type background and generates body morphology defects. Transgene and status as a rescue of *pat-2(st567)* or wild type background is listed on each image. Arrows indicate actin filaments. Scale bar, 25 μm.

TABLE 1

INTACT AND CHIMERIC *INA-1* INTEGRINS RESCUE A LETHAL *INA-1* ALLELE

Transgene	% Rescued	Lines analyzed	n
ina-1	99.5 +/− 0.002	2	829
ina-1(pat-2cyto)	98.7 +/− 0.004	4	851

Rescue was determined for *ina-1(gm86)* homozygous individuals by subtracting the number of L1 arrested larval from the total progeny then dividing by the total progeny, similar to the approach used by Martin-Bermudo *et al.*, (1997). Only Venus expressing progeny were evaluated. At least 3 experiments were performed for each line.

TABLE 2

PARTIAL RESCUE OF A *PAT-2* LETHAL ALLELE BY A CHIMERIC INTEGRIN

Transgene	% Rescued	Lines analyzed	n
pat-2	99.5 +/− 0.54	3	468
pat-2(ina-1cyto)	54.0 +/− 9.2*	4	515

Rescue was determined for *unc-79(e1068), pat-2(st567)* homozygous individuals by subtracting the number of Pat embryos from the total progeny then dividing by the total progeny, similar to the approach used by Martin-Bermudo *et al.*, (1997). Only Venus expressing progeny were evaluated. At least 3 experiments were performed for each line. Asterisk indicates p value < 0.05.

TABLE 3

CHIMERIC INTEGRINS CAUSE DTC MIGRATION DEFECTS

Transgene	Genetic background	% DTC migration defects	Lines	n
ina-1	*ina-1(gm86)*	5.4 +/−1.2*	4	178
ina-1(pat-2cyto)	*ina-1(gm86)*	24.8 +/−2.5*	3	460
pat-2	*pat-2(st567)*	8.6 +/−2.2	3	200
pat-2(ina-1cyto)	*pat-2(st567)*	9.3 +/−2.7	2	160
pat-2	WT	8.0 +/−1.8*	3	108
pat-2(ina-1cyto)	WT	19.9 +/−1.0*	3	302

Averages were generated from at least 3 independent experiments. Genetic background was homozygous. Asterisk indicates p value < 0.05 for comparison of *ina-1* to *ina-1(pat-2cyto)* and *pat-2* WT background to *pat-2(ina-1cyto)* WT background.